Discrete cosine transform domain restoration of defocused images

Edmund Y. Lam and Joseph W. Goodman

In discrete-cosine-transform-based (DCT-based) compressions such as JPEG it is a common practice to use the same quantization matrix for both encoding and decoding. However, this need not be the case, and the flexibility of designing different matrices for encoding and decoding allows us to perform image restoration in the DCT domain. This is especially useful when we have severe limitations on the computational power, for instance, with in-camera image manipulation for programmable digital cameras. We provide an algorithm that compensates partially for a defocus error in image acquisition, and experimental results show that the restored image is closer to the in-focus image than is the defocused image. © 1998 Optical Society of America

OCIS codes: 100.3020, 110.6980, 220.1000, 220.2560, 110.4280.

1. Introduction

The JPEG algorithm is a very popular lossy image-compression standard for still-frame, continuous-tone images.[1] In this algorithm the image is first divided into 8×8 pixel nonoverlapping blocks, and each block is subjected to a discrete cosine transform (DCT). The coefficients are then quantized according to the quantization matrix Q_e. This is done by the rounding-off of the quotients when the DCT coefficients are divided entrywise by Q_e. They are then entropy coded before transmission. On receiving the encoded coefficients, the decoder reverses the process for the entropy coding, dequantizes the coefficients by multiplication entrywise with the matrix Q_d, and performs the inverse DCT. The compression is lossy because of the quantization process.

It is customary and convenient to use the same quantization matrix for both encoding and decoding, i.e., $Q_e = Q_d$. The JPEG committee actually recommends the matrix shown in Fig. 1 for both Q_e and Q_d that takes into account some of the human visual system properties, although its use is strictly voluntary. In the literature one can find various attempts to vary the dequantization matrix Q_d slightly to achieve better images (see, for example, Refs. 2, 3, and 4). In this paper we first show that using $Q_e = Q_d$ is not necessarily optimal in terms of reducing noise, and, in fact, in some circumstances the flexibility of using a Q_e different from Q_d allows us to restore images in the DCT domain. In particular, we provide an algorithm for image restoration when the image has been taken out of focus. We assume here that the amount of focusing error is known *a priori* or estimated beforehand by some external means. We show that, after compression and decompression, the image is closer (in the mean-square sense) to the original in-focus image than is the uncompressed defocused image.

Before we proceed, however, it is imperative for us to explain why and when this algorithm would be useful. The motivation behind the scheme is that, as the sensors in digital cameras move from being CCD-based to complementary metal-oxide semiconductor-based, it is possible to allow a certain amount of computational power in the camera to be devoted to image restoration. For example, instead of mechanically moving the lens to adjust focusing, we can use the computational capacity to manipulate the image concurrently, thereby reducing the need for exact positioning of the lens. However, the cost of in-camera computation is much more expensive than if done off-line, and a full-frame fast Fourier transform of the image is not desirable because its complexity goes up too rapidly with the size of the image. Yet, as most cameras have built-in JPEG compression and decompression algorithms in place, it would be quite cost effective if we could take advantage of the blockwise DCT that is readily avail-

The authors are with the Information Systems Laboratory, Stanford University, Stanford, California 94309.

Received 21 April 1998; revised manuscript received 24 June 1998.
0003-6935/98/266213-06$15.00/0

16	11	10	16	24	40	51	61
12	12	14	19	26	58	60	55
14	13	16	24	40	57	69	56
14	17	22	29	51	87	80	62
18	22	37	56	68	109	103	77
24	35	55	64	81	104	113	92
49	64	78	87	103	121	120	101
72	92	95	98	112	100	103	99

Fig. 1. Recommended JPEG quantization matrix.

able to us as part of the JPEG standard. Our goal therefore is to make use of the blockwise DCT frequency components in the design of Q_e and Q_d to approximate the desired image restoration had we been able to perform the full-frame fast Fourier transform.

2. Noise Trade-Off

Consider one 8×8 pixel block of the image. Let its DCT-domain representation be $X(u, v)$, where u and v are the spatial frequencies in the horizontal and the vertical directions, respectively, both ranging from 0 to 7. Using $X_q(u, v)$ to denote the quantized coefficients and $X_n(u, v)$ for the quantization noise, we see that they are related by

$$\frac{X(u, v)}{Q_e(u, v)} = X_q(u, v) + X_n(u, v). \tag{1}$$

Because we transmit only $X_q(u, v)$, for decoding we have

$$\hat{X}(u, v) = Q_d(u, v)X_q(u, v), \tag{2}$$

where we use $\hat{X}$ to denote the estimate of X. Now, to compare the original and the decompressed images, we normally would have to calculate the mean-square error (MSE) in the space domain. However, because of the unitary nature of the type II two-dimensional DCT used in JPEG, we could employ the Parseval theorem and perform the calculation in the DCT domain.[4] Therefore

$$\begin{aligned} \mathrm{MSE} &= \sum_{u=0}^{7} \sum_{v=0}^{7} [X(u, v) - \hat{X}(u, v)]^2 \\ &= \sum_{u=0}^{7} \sum_{v=0}^{7} [(Q_e - Q_d)X_q + Q_e X_n]^2, \end{aligned} \tag{3}$$

where it is understood that Q_e, Q_d, X_q, and X_n all have arguments (u, v). We can see that, when X_n is small and X_q is large, it is reasonable to set $Q_e = Q_d$ to generate a small MSE. However, typically for high frequencies we have larger X_n and smaller X_q, and changing Q_e at those frequencies would provide a trade-off between the sources of noise and might reduce the overall MSE. With this in mind, we now look at a specific case in which the original image is, in fact, corrupted by an out-of-focus optical transfer function (OTF), and we modify the quantization matrix Q_e to perform partial restoration.

3. Defocusing

When imaging a diffraction-limited system with incoherent light, the object and the image are related by[5]

$$\mathcal{G}_i(f_x, f_y) = \mathcal{H}(f_x, f_y)\mathcal{G}_g(f_x, f_y), \tag{4}$$

where $\mathcal{G}_i$ is the normalized frequency spectrum of the image intensity I_i, $\mathcal{G}_g$ is the normalized frequency spectrum of the object intensity I_g, and $\mathcal{H}$ is the OTF. If the ideal focusing plane is at z_i from the lens but we focus on z_a and the radius in the pupil is r, we define, as in Ref. 5,

$$W_m = \frac{1}{2}\left(\frac{1}{z_a} - \frac{1}{z_i}\right)r^2, \tag{5}$$

which is an indication of the severity of the focusing error when normalized by the wavelength λ. The path-length error is therefore

$$W(x, y) = W_m \frac{x^2 + y^2}{r^2}, \tag{6}$$

and we can express the OTF as

$$\mathcal{H}(f_x, f_y) = \frac{\displaystyle\iint_{\mathcal{A}(f_x, f_y)} \exp\{jk[W(x + x_0, y + y_0) - W(x - x_0, y - y_0)]\}\mathrm{d}x\mathrm{d}y}{\displaystyle\iint_{\mathcal{A}(0,0)} \mathrm{d}x\mathrm{d}y}, \tag{7}$$

where $\mathcal{A}(f_x, f_y)$ is the area of overlap of the pupil displaced by $\pm(x_0, y_0)$ and

$$x_0 = \frac{\lambda z_i f_x}{2}, \qquad y_0 = \frac{\lambda z_i f_y}{2}. \tag{8}$$

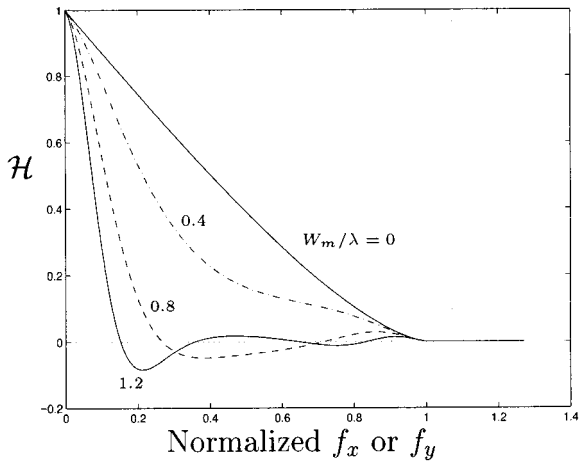

Fig. 2. Cross-sectional view of the OTF.

Figure 2 shows a cross section of the OTF for a circular pupil with various amounts of defocus. We see that, even for in-focus imagery, we have a cutoff because of the finite size of the pupil and we also see attenuation at frequencies before the cutoff. For restoration of a defocused image, our goal is to modify it to resemble the in-focus image rather than to reproduce the object itself.

4. Discrete Cosine Transform-Domain Restoration

Because the OTF multiplies the Fourier transform of the images, we expect the middle to high frequencies (where the OTF's of $W_m/\lambda = 0$ and $W_m/\lambda > 0$ differ most) to be more severely suppressed, and ideally we would like to boost those frequencies. However, in the DCT domain the blockwise frequencies do not bear a simple relation to the frequency components in the Fourier domain. Indeed, blocking destroys the space invariance of the system, so we cannot relate the object and the image by a transfer function, as in Eq. (4). Therefore it is not possible to specify analytically the amount of preemphasis required for each of the DCT frequency components from the OTF's that are expressed in the Fourier domain. Instead, we collect a set $\mathscr{C}_{\text{in}}$ of in-focus images and another set $\mathscr{C}_{\text{out}}$ of the corresponding out-of-focus images. Let $X_{\text{in}}(u, v)$ be the vector containing the (u, v) DCT coefficients in all the blocks of the in-focus images and $X_{\text{out}}(u, v)$ be the corresponding vector for the out-of-focus images. We then seek a multiplicative factor such that

$$X_{\text{out}}(u, v)a(u, v) \approx X_{\text{in}}(u, v). \tag{9}$$

The best value for $a(u, v)$, in the mean-square sense, is given by

$$a(u, v) = \frac{\langle X_{\text{in}}(u, v), X_{\text{out}}(u, v)\rangle}{\langle X_{\text{out}}(u, v), X_{\text{out}}(u, v)\rangle}, \tag{10}$$

where $\langle \cdots \rangle$ denotes the inner product. This method is related to the variance-matching method described in Ref. 6 that is designed for text sharpening in scanned images, but it is superior in terms of the MSE reduction. In Appendix A we provide an examination of when the variance-matching method converges to the minimum MSE method used here. Unfortunately, we have no guarantee that $a > 0$, and, indeed, it might not be if its calculation is dominated by noise. Therefore we clip a to be ≥ 0.001. Note that we do not have to multiply the DCT coefficients by $a(u, v)$ before quantization but can simply change the encoding quantization matrix to

$$Q_e(u, v) = \frac{Q(u, v)}{a(u, v)}, \tag{11}$$

where Q could be the quantization matrix shown in Fig. 1.

-1	-1	-1
-1	8	-1
-1	-1	-1

Fig. 3. Laplacian convolution kernel.

5. Regularization

Because of the ill-posed nature of the image-restoration problem, a minimum MSE solution is known to be highly sensitive to noise, especially at high frequencies.[7] It is very important to incorporate some regularization constraint to compromise between the fidelity of the data and consistency with *a priori* knowledge of the image. Here we propose a method of regularization similar to that reported in Ref. 4 that can be incorporated in the dequantization matrix Q_d.

Assume that we have B blocks altogether. Let $l(j, k)$ be a high-pass filter, such as that of a Laplacian kernel, as shown in Fig. 3.[8] Let L be the two-dimensional discrete Fourier transform of l with a size of 8×8 pixels, so

$$G_i = \sum_{u=0}^{7} \sum_{v=0}^{7} [X_{\text{in}}(u, v)L(u, v)]^2 \tag{12}$$

would measure the amount of high-frequency content in block i. Therefore we want

$$\sum_{u=0}^{7} \sum_{v=0}^{7} [\hat{X}_{\text{out}}(u, v)L(u, v)]^2 \leq G = \frac{1}{B} \sum_{i=1}^{B} G_i. \tag{13}$$

Expression (13) serves as our regularization constraint. At the same time, we also want to constrain

Fig. 4. (a) In-focus image. (b) Defocused image. (c) Image compressed and decompressed with the normal Q. (d) Image compressed and decompressed with the improved Q_e and Q_d.

the MSE of the reconstructed image compared with the in-focus image. Therefore we have

$$\sum_{u=0}^{7}\sum_{v=0}^{7}\left[\frac{\hat{X}_{\text{out}}(u,v)}{Q(u,v)}-X_{q,\text{out}}\right]^2 \le R = \frac{1}{B}\sum_{i=1}^{B}\left[\sum_{u=0}^{7}\sum_{v=0}^{7}X_{n,\text{in}}{}^2(u,v)\right]. \tag{14}$$

The term on the left-hand side of expression (14) is our objective function, and our goal is to minimize it subject to the constraints mentioned above. Having set up the optimization problem, we can now solve it by means of a Lagrangian multiplier. Therefore we have

$$J(\nu)=\sum_{u=0}^{7}\sum_{v=0}^{7}\left[\frac{\hat{X}_{\text{out}}(u,v)}{Q(u,v)}-X_{q,\text{out}}\right]^2 + \nu\sum_{u=0}^{7}\sum_{v=0}^{7}[\hat{X}_{\text{out}}(u,v)L(u,v)]^2, \tag{15}$$

Table 1. Values of the SNR for Various Images

Conditions	SNR Without Noise	SNR With Noise
Before compression	25.1 dB	24.3 dB
With the standard $Q_e = Q_d$	23.4 dB	23.2 dB
With customized Q_e and Q_d	25.9 dB	25.1 dB

where we use ν to represent the Lagrangian to avoid confusion with the wavelength λ. As discussed in Refs. 9 and 10, ν is given by (R/G). Now, by setting

$$\frac{\partial J(\nu)}{\partial \hat{X}_{\text{out}}} = 0, \tag{16}$$

we obtain, after some simplification,

$$\hat{X}_{\text{out}}(u, v) = \frac{Q(u, v)G}{G + Q^2(u, v)L^2(u, v)R} X_{q,\text{out}}. \tag{17}$$

Compared with Eq. (2), it is clear that we should set Q_d to

$$Q_d(u, v) = \frac{Q(u, v)G}{G + Q^2(u, v)L^2(u, v)R}. \tag{18}$$

Note that, as $G \to \infty$, i.e., as we relax the regularization constraint, we obtain $Q_d = Q$. Finally, we need to round Q_d off to contain integers in the range of 0 to 255, because the entries of the quantization matrix are represented as 8-bit unsigned integers in the JPEG algorithm.[1]

6. Simulation Results

We implement the algorithm on a 256×256 pixel "bridge" image, and the resulting images are shown in Fig. 4. To obtain a quantitative comparison among the images, we use the signal-to-noise ratio (SNR) as the metric. The SNR is defined as[11]

$$\text{SNR}(x, \hat{x}) = 10 \log_{10} \left\{ \frac{\sum_j \sum_k [x(j, k)]^2}{\sum_j \sum_k [x(j, k) - \hat{x}(j, k)]^2} \right\}, \tag{19}$$

where (j, k) range over the whole image. Figure 4(a) shows the ideal in-focus image that we would like to obtain with an aberration-free lens. Figure 4(b) shows the image we get with the defocus parameter $W_m/\lambda = 0.4$. We also add some Gaussian noise to the defocused image, with SNR = 30 dB. We compress and decompress the image of Fig. 4(b) with the standard quantization matrix as is recommended by the JPEG standard (see Fig. 1) to arrive at Fig. 4(c). On the basis of this quantization table, we make changes in accordance with our algorithm outlined above for Q_e and Q_d, and we obtain the image shown in Fig. 4(d). We also did a set of experiments in which no noise was present, and the SNR's of these two sets of experiments are listed in Table 1. We note that our method generally yields a higher SNR than even the uncompressed defocused image.

7. Conclusions

In this paper we have presented an algorithm that takes advantage of the flexibility in designing the quantization matrices of the JPEG to perform partial restoration of images. The experimental results show that the restored images, although quantized, could have less distortion in terms of the MSE compared with the unquantized images before processing.

Appendix A

In the variance-matching method,[6] the multiplicative factor $a'(u, v)$ is chosen such that

$$a'(u, v) = \left[\frac{\text{Var}(X_{\text{in}})}{\text{Var}(X_{\text{out}})} \right]^{1/2} = \left[\frac{\frac{1}{n} \sum X_{\text{in}}{}^2 - \left(\frac{1}{n} \sum X_{\text{in}} \right)^2}{\frac{1}{n} \sum X_{\text{out}}{}^2 - \left(\frac{1}{n} \sum X_{\text{out}} \right)^2} \right]^{1/2}, \tag{A1}$$

and we want to compare it against our calculation of a in Eq. (10). From the Cauchy–Schwarz inequality we know that

$$\left(\sum X_{\text{in}} X_{\text{out}} \right)^2 \le \sum X_{\text{in}}{}^2 \sum X_{\text{out}}{}^2, \tag{A2}$$

with equality if and only if X_{out} equals X_{in} or a scaled version of it. Now, by taking the square root on both sides and rearranging the terms in Eq. (A2), we obtain

$$\frac{\sum X_{\text{in}} X_{\text{out}}}{\sum X_{\text{out}}{}^2} \le \left(\frac{\frac{1}{n} \sum X_{\text{in}}{}^2}{\frac{1}{n} \sum X_{\text{out}}{}^2} \right)^{1/2}. \tag{A3}$$

Except for the dc frequency, X_{in} and X_{out} are reasonably approximated to possess zero-mean Laplacian distributions,[12] so we have $1/n \sum X_{\text{in}} \approx 0$ and $1/n \sum X_{\text{out}} \approx 0$, and Eq. (A3) now implies that $a \le a'$. Because X_{out} is generally not simply a scaled version of X_{in}, the variance-matching algorithm tends to overcompensate the defocus by selecting a value of $a' > a$.

References

1. W. Pennebaker and J. Mitchell, *JPEG Still Image Data Compression Standard* (Van Nostrand Reinhold, New York, 1992).
2. R. Brown and A. Boden, "*A posteriori* restoration of block transform-compressed data," in *1995 Proceedings of the Data Compression Conference*, J. A. Storer and M. Cohn, eds. (IEEE Computer Society Press, Los Alamitos, Calif., 1995), p. 426.
3. Z. Fan and R. Eschbach, "JPEG decompression with reduced artifacts," in *Image and Video Compressions*, M. Rabbani and R. J. Safranek, eds., Proc. SPIE **2186,** 50–55 (1994).
4. R. Prost, Y. Ding, and A. Baskurt, "JPEG dequantization array

for regularized decompression," IEEE Trans. Image Process. **6,** 883–888 (1997).
5. J. W. Goodman, *Introduction to Fourier Optics*, 2nd ed. (McGraw-Hill, New York, 1996).
6. V. Bhaskaran, K. Konstantinides, and G. Beretta, "Text and image sharpening of scanned images in the JPEG domain," in *Proceedings of the Fourth IEEE International Conference on Image Processing* (Institute of Electrical and Electronics Engineers, New York, 1997), Vol. 2, pp. 326–329.
7. G. Demoment, "Image reconstruction and restoration: overview of common estimation structures and problems," IEEE Trans. Acoust. Speech Signal Process. **37,** 2024–2036 (1989).
8. K. R. Castleman, *Digital Image Processing* (Prentice Hall, Englewood Cliffs, N.J., 1996).
9. M. G. Kang and A. K. Katsaggelos, "General choice of the regularization functional in regularized image restoration," IEEE Trans. Image Process. **4,** 594–602 (1995).
10. K. Miller, "Least-squares methods for ill-posed problems with a prescribed bound," SIAM J. Math. Anal. **1,** 52–74 (1970).
11. A. K. Jain, *Fundamentals of Digital Image Processing* (Prentice Hall, Englewood Cliffs, N.J., 1989).
12. R. Reininger and J. Gibson, "Distributions of the two-dimensional DCT coefficients for images," IEEE Trans. Commun. **COM-31,** 835–839 (1983).